The effect of fibre volume fraction on the onset of fracture in laminar materials with an array of coplanar interface cracks

Bartlomiej Winiarski, Igor A. Guz

The effect of fibre volume fraction on the onset of fracture in laminar materials with an array of coplanar interface cracks

Bartlomiej Winiarski, Igor A. Guz

PII: S0266-3538(07)00299-0
DOI: 10.1016/j.compscitech.2007.08.001
Reference: CSTE 3790

To appear in: *Composites Science and Technology*

Received Date: 24 April 2007
Revised Date: 6 July 2007
Accepted Date: 2 August 2007

Please cite this article as: Winiarski, B., Guz, I.A., The effect of fibre volume fraction on the onset of fracture in laminar materials with an array of coplanar interface cracks, *Composites Science and Technology* (2007), doi: 10.1016/j.compscitech.2007.08.001

THE EFFECT OF FIBRE VOLUME FRACTION ON THE ONSET OF FRACTURE IN LAMINAR MATERIALS WITH AN ARRAY OF COPLANAR INTERFACE CRACKS

Bartlomiej Winiarski, Igor A. Guz*

Centre for Micro- and Nanomechanics (CEMINACS)

College of Physical Sciences, University of Aberdeen

Fraser Noble Building, Aberdeen AB24 3UE, Scotland, U.K.

tel. +44 (0) 1224 272808, e-mail: i.guz@abdn.ac.uk

Abstract. The onset of fracture process in a layered composite with coplanar interface cracks under compression along layers is studied within the scope of 3-D theory of stability using the model of piecewise-homogeneous medium. Each layer consists of a matrix reinforced by continuous parallel fibres and is modelled by a compressible, linear elastic, transversely isotropic material. The eigenvalue problem with respect to the controlled parameters, namely, the crack length, the crack spacing and the *0°*-plies layer volume fraction is solved for the shear and the extensional modes utilizing the finite element analysis by commercially available FE code. The results are obtained for *0°*-plies volume fraction $V_{0°}$=0.1…0.9 for the typical dispositions of cracks. The effect of the crack length, the crack spacing and the *0°*-plies volume fraction on the critical microbuckling strain in the composite was determined.

Keywords: layered structure, interlaminar defects, fracture, buckling, finite element analysis (FEA)

* Corresponding author

1. Introduction

The use of composite materials in the aviation sector is increasingly important as efficiency is improved through lighter, more aerodynamic components, higher corrosion resistance, increased service life and reduced maintenance requirements. Complex integral components with composites are leading to further weight reduction through less joining and fewer parts. Layered composite materials with aluminium-lithium alloys, epoxy resin and high strength carbon fibre systems are used in the aviation and aerospace industries to build light, strong components with high fatigue resistance in particular as primary structures. These structures contain wide range of intra- and interlaminar defects formed during fabrication process or in-service. The classical Griffith-Irvin criterion of linear fracture mechanics or its generalizations are inapplicable for laminated composites compressed along interlaminar defects located in the symmetry planes, since in such case all stress intensity factors are equal to zero due to the specific loading conditions. The beginning of fracture process under compression is very often associated with the buckling in the microstructure of the material, the internal or the surface instabilities phenomena according to Biot [1] and Guz [2, 3], when the critical load is determined by parameters characterising the microstructure of the composite rather then by the dimensions and shape of the specimen or structural element. In this paper the following concept of fracture is adopted: the onset of fracture coincides with local loss of stability of the equilibrium state of the material that surrounds the crack. Of course, internal instability does not always cause the ultimate material failure. To fully investigate the problem of compressive failure, the postcritical behaviour must also be analysed.

The accurate (exact) approach to study this phenomenon is based on the model of a piecewise-homogeneous medium, when each component of the material is described as the three-dimensional object provided certain boundary conditions are satisfied at the interfaces.

In the literature one can find only the first step on the way to the exact solution of the problem of stability in compression for composites with interlaminar defects. The classification of cracks was introduced and the bounds for critical loads were suggested and substantiated by Guz [4, 5], Guz and Soutis [6, 7], Soutis and Guz [8], and Guz and Herrmann [9]. These works also contain the reviews of the existing simplified models, which are not analysed in this paper. There are also numerous publications devoted to compressive strength of layered materials without defects, i.e. with perfect bonding for all interfaces between the layers. The detailed reviews of different methods of modelling it were given, for example, by Budiansky and Fleck [10], Guz [2, 3], Soutis [11], Guz et al [12], Soutis and Turkmen [13], Talreja [14], and Waas and Schultheisz [15].

The current paper addresses the problem of modelling the onset of fracture process due to internal instability (microbuckling) under static compression along layers in a laminar composite with a specific set of defects, namely a periodic array of coplanar interfacial cracks.

2. Problem statement

The layered composite with interlaminar cracks is described within the analytical model and the classification of cracks proposed by Guz [4]. The composite under consideration consists of alternating layers. An array of cracks is located on the different coplanar interfaces. Here we consider two possible cases: a periodic array of cracks, Fig. 1a, and two cracks (structural cracks according to Guz [4]), Fig. 1b.

The layers are simulated by compressible elastic transversely isotropic solids (a matrix reinforced by continuous parallel fibres) in continuum approximation. The principal material directions are perpendicular and parallel to the interfaces. Henceforth all values referred to these layers will be labelled by indices '*r*' (*0°*-plies) and '*m*' (*90°*-plies). The composite is

situated in condition of plane strain state in compression along layers by 'dead' loads applied at infinity in such a manner that equal deformations along all layers are provided in the direction of loading, i.e. $\varepsilon_{22}^{0(r)} = \varepsilon_{22}^{0(m)}$, $\sigma_{22}^{0(r)} \neq \sigma_{22}^{0(m)}$. This is a uniform precritical state. Hereafter *'0'* means precritical state.

In this paper the concept of fracture is adopted following Biot [1] and Guz [3]: the onset of fracture coincides with local loss of stability of the equilibrium state of the material that surrounds the crack.

The stability problem is formulated by using the fundamental relationships of the three-dimensional theory of stability given by Guz [3], and the model of a piecewise-homogeneous medium (the exact statement). All the equations below are formulated for perturbation of stresses (t_{ij}), which are components of a non-symmetric Kirchhoff stress tensor, and displacements (u_i). In so doing, the static method of investigation of static problems of 3-D theory of stability can be used, since the conditions sufficient for the applicability of this method were proved to be satisfied in the case of compression by 'dead' loads [3].

The stability equations for each of the layers are

$$\frac{\partial}{\partial x_i}\left(t_{ij}^{(r)}\right) = 0; \quad \frac{\partial}{\partial x_i}\left(t_{ij}^{(m)}\right) = 0; \qquad i, \ j = 1, \ 2 \tag{1}$$

The stress and displacement perturbations are related as

$$t_{ij}^{(r)} = \omega_{ij\alpha\beta}^{(r)} \frac{\partial u_\alpha^{(r)}}{\partial x_\beta}; \quad t_{ij}^{(m)} = \omega_{ij\alpha\beta}^{(m)} \frac{\partial u_\alpha^{(m)}}{\partial x_\beta}; \qquad i, \ j, \ \alpha, \ \beta = 1, \ 2 \tag{2}$$

The components of $\boldsymbol{\omega}$ tensor depend on the material properties and on the load [3].

The layer interfaces for the case of periodic array of cracks consist of zones of perfectly bonded layers (S_{pb})

$$S_{pb} = \left[\begin{array}{l} \left(0 \ge x_2 \ge a; \;\; x_1 = n(h+H) \right) \cup \\ \cup \left((b+a) \le x_2 \le b; \;\; x_1 = h + n(h+H) \right), \;\; n = \pm 0,\; 1,\; 2,\; \ldots \end{array} \right] \tag{3}$$

and cracks (S_{cr})

$$S_{cr} = \left[\begin{array}{l} \left(0 < x_2 < a; \;\; x_1 = n(h+H) \right) \cup \\ \cup \left((b+a) > x_2 > b; \;\; x_1 = h + n(h+H) \right), \;\; n = \pm 0,\; 1,\; 2,\; \ldots \end{array} \right] \tag{4}$$

For the case of two cracks, Eq. (3) and (4) can be re-written as

$$S_{pb} = \left[\left(0 \ge x_2 \ge a; \;\; x_1 = 0 \right) \cup \left((b+a) \le x_2 \le b; \;\; x_1 = h \right) \right] \tag{5}$$

$$S_{cr} = \left[\left(0 < x_2 < a; \;\; x_1 = 0 \right) \cup \left((b+a) > x_2 > b; \;\; x_1 = h \right) \right] \tag{6}$$

Since the crack surfaces are free of stresses since the initial moment of stability loss, but not the postcritical behaviour, is considered in the present study. Therefore the conditions for stresses are

$$t_{11}^{(r)} = 0; \;\; t_{11}^{(m)} = 0; \;\; t_{12}^{(r)} = 0; \;\; t_{12}^{(m)} = 0; \;\; \text{if} \;\; (x_1, x_2) \in S_{cr} \tag{7}$$

On the interfaces with perfect bonds the conditions of stress and displacement continuity are fulfilled:

$$t_{11}^{(r)} = t_{11}^{(m)}; \;\; t_{12}^{(r)} = t_{12}^{(m)}; \;\; u_1^{(r)} = u_1^{(m)}; \;\; u_2^{(r)} = u_2^{(m)} \;\; \text{if} \;\; (x_1, x_2) \in S_{pb} \tag{8}$$

Besides that, the condition of the attenuation of perturbations when moving away from the cracks must be satisfied for the periodic array of cracks (Fig. 1a) in the form:

$$u_2^{(r)}\Big|_{x_2 \to \infty} \to 0; \;\; u_2^{(m)}\Big|_{x_2 \to \infty} \to 0 \tag{9}$$

and for two cracks (Fig. 1b):

$$u_i^{(r)}\Big|_{x_i \to \infty} \to 0; \;\; u_i^{(m)}\Big|_{x_i \to \infty} \to 0; \quad i = 1,\; 2 \tag{10}$$

Equations (1) - (10) constitute an eigenvalue problem which will be solved below using the finite element (FE) method.

3. Numerical analysis

In order to solve the above-stated problem, the commercially available FE code, ABAQUS [16], was used to conduct the numerical analysis. The FE model assembly of the composite structure, asymmetry planes (the shear mode) and symmetry planes (the extensional mode) are shown in Fig. 1a for the periodic array of cracks and in Fig. 1b for two coplanar cracks, together with the global coordinate system. The model contains three parts, namely L, C and R. The local coordinate systems for each part are compatible with the global coordinate system. The crack length a is related to lamina thickness by parameter a/h ('the crack length'). The crack spacing is characterised by parameter b/a ('the crack spacing'). The experimental engineering constants for each layer (the parts L, R and C) are shown in Table 1.

On the interfaces with perfect bonds the conditions of stresses and displacements continuity, Eq. (5), are implemented. The plane strain condition in compression along layers, Eq. (1), is imposed. In order to capture the lowest buckling mode the stress free faces of cracks, Eq. (4), are regarded as free surfaces. It should be noted this assumption can be imposed on the condition that a precritical state is considered.

The convergence of FE solution to the exact solution was examined by means of *p*-convergence and *h*-convergence procedures following Fung and Tong [17]. The convergence analysis was performed for the three types of elements: linear triangular (*CPE3*), linear quadrilateral (*CPE4*) and square quadrilateral (*CPE8*) and for the number of elements along crack face in the range from 5 to 180. In order to fulfil the conditions given by Eqs. (9) and (10), a numerical experiment was performed.

All three parts were modelled by 6-nodes and 8-nodes plane strain elements, namely *CPE6M* and *CPE8* with minimum of 20 elements along cracks face. The cross-section of part C contains minimum of 8 elements in the vicinity of cracks. The numbers of elements for the chosen models are shown in Table 2. The numbers of elements for other models are within the same range. The parameters were chosen because they represent a reasonable choice between a good accuracy of the results (<3%) and computational time. Fig. 2 shows the mesh pattern in the vicinity of cracks.

4. Results of FE analysis.

The results of eigenvalue analysis for different volume fractions of *0°*-plies are given in Figs. 3 and 4. Fig. 3 shows the critical strain, ε_{cr}, versus *0°*-plies volume fraction, $V_{0°}$, for different crack lengths, *a/h*, and different crack spacing, *b/a*, for the case of shear mode. Fig. 4 shows similar dependencies for the extensional mode. In addition, Figs. 3 and 4 contain the results for the model of two structural cracks [18]. The cases A and B for the model of two structural cracks (Fig. 1b) represent a very low volume fraction of *0°*-plies and a very high volume fraction of *0°*-plies, respectively. The highest critical strains (2.78 %) coincide with the critical strain value for microcrack calculated analytically according to Guz [3] and Guz et al [20]. It confirms the validity of the FE model. The lines ε_{cr}=1.53% and ε_{cr}=1.06%, reflect the experimental critical strains for graphite-epoxy composite compressed in the direction perpendicular to, and along the fibres, respectively [21].

Two well defined buckling instability regions are distinguishable in Figs. 3 and 4. The first one is the 'microcrack-like' buckling region, where the crack length *(a/h)*, the crack spacing *(b/a)* and the *0°*-plies volume fraction *($V_{0°}$)* do not influence the critical strain. The critical strain for considered layered composite compressed along the interface - for *a/h*<0.1 and

$b/a \geq 0$ - is independent of the number and disposition of cracks at the interface, regardless of the mode of stability loss, and coincides with the critical strain for one microcrack on the interface [19]. In this case, the surface stability loss phenomenon occurs, see Biot [1] and Guz [3]. The maximum crack length, when surface instability can occur, is described by parameter $(a/h)_{cr}$ for a given $b/a<1$ [18]:

$$(a/h) \cong (a/h)_{cr}\big|_{b/a<1} \quad if \quad \frac{\varepsilon_{cr}^{mc.} - \varepsilon((a/h)_{cr})}{\varepsilon_{cr}^{mc.}} \to 1\% \tag{11}$$

where $\varepsilon_{cr}^{mc.}$ is the critical strain for microcrack.

In the second region, the crack length *(a/h)*, the crack spacing *(b/a)* and the 0°-plies volume fraction (V_{0°) do influence the critical strain. In this case the internal stability loss phenomenon occurs; see Biot [1] and Guz [3]. The increase in the crack length, for $a/h>0.1$, causes the decrease in the critical strain, for the given crack spacing. The increase in the crack spacing, within the range $0<b/a<1$, causes the increase in the critical strain for the given crack length. The internal instability phenomenon occurs in the 0°-plies and in the 90°-plies for the case A and B for the model of two structural cracks (Fig. 1b), respectively. The magnitude of the effect of crack length on critical strain is described by the parameter $\delta_{\varepsilon max}$ [18]:

$$\delta_{\varepsilon \max} = \max\left(\frac{\partial^2 \varepsilon_{cr}}{\partial (a/h)^2}\bigg|_{(b/a=0)} \right) \tag{12}$$

The transition regions between the above mentioned instability phenomena are described by the following set of parameters for a certain combination of *b/a* and *a/h* [18]:

$$[(a/h)_{cr}; (a/h)_{\max}]; \quad where \quad (a/h)_{\max} = f(\delta_{\varepsilon \max}) \tag{13}$$

Within the transition region, any of the two competing mechanisms of stability loss can occur.

Fig. 3 clearly shows that the 0°-plies volume fraction influences the critical strain level for shear mode of stability loss. The results for very low 0°-plies volume fractions, i.e. $V_{0^\circ}<0.01$, and very high 0°-plies volume fractions, i.e. $V_{0^\circ}>0.99$, converge to the results for two

structural cracks (Fig. 1b). In this case, the laminar composite with periodic array of interfacial cracks can be modelled as a single thin layer between two dissimilar half-planes with two cracks on two interfaces adjacent to the thin layer, since there is no interaction between the pairs of coplanar cracks. The internal instability phenomenon occurs in the *0°*-plies and in the *90°*-plies for very low and very high volume fractions of *0°*-plies, respectively. Here, the buckling pattern contains the series of isolated buckling regions, where two nearest cracks interact, see the in-plane principal strain distributions obtained by FEA, Fig. 5.

For a single buckling region, the internal instability phenomenon always occurs inside the region of *0°*-plies or *90°*-plies described by the set of the following parameters:

$$\left(h, a_{cr}\right)\Big|_{b/a<1}, \quad where \quad a_{cr} = \frac{a-b}{h}; \quad b/a < 1 \tag{14}$$

The distance between the isolated buckling regions is H. The shear mode for the laminar composite contains a well pronounced extremum of the critical strain, particularly for the crack length $a/h>1$. The minimum of critical strain is reached for the *0°*-plies volume fraction $V_{0^\circ}=0.5$. The occurrence of the extremum is related to formation of the microbuckling band due to the multiple crack interaction; see the in-plane principal strain distributions obtained by FEA, Fig. 6. Here, the influence of the crack spacing on variation of the critical strain is weak and for the *0°*-plies volume fraction $V_{0^\circ}=0.7...0.8$ the critical strains for $b/a=0$, $b/a=0.8$ and $a/h=15$ are essentially the same.

The results for extensional mode of stability loss are given in Fig. 4. In the case of $b/a=0$, the *0°*-plies volume fraction from the ranges $0.01<V_{0^\circ}<0.4$ and $0.7<V_{0^\circ}<0.99$ does not influence the critical strain level, and the results converge well with the results for two structural cracks [18]. The buckling pattern contains the series of isolated buckling regions, where two nearest cracks interact; see the in-plane principal strain distributions obtained by FEA, Fig 7. The buckling region is defined by set of parameters (h, a_{cr}). In the case of

b/a=0.8, the influence of the 0°-plies volume fraction from the ranges $0.01<V_{0^\circ}<0.4$ and $0.7<V_{0^\circ}<0.99$ on the variation of critical strain level is noticeable. However, the dependence is rather weak for short cracks, $a/h < 2$; see also [19]. The internal instability phenomenon occurs in the 0°-plies for the layer volume fraction $V_{0^\circ}<0.4$ and in the 90°-plies for the layer volume fraction $V_{0^\circ}>0.6$. The critical strain level for the 0°-plies volume fraction $0.45<V_{0^\circ}<0.6$ increases rapidly due to the change of the buckling region from 0°-plies to 90°-plies for the given crack length and the crack spacing; see the in-plane principal strain distributions obtained by FEA, Figs. 8a and 8b.

Taking into account the lines ε_{cr}= 1.53% and ε_{cr}= 1.06%, we can say that for the periodic array of cracks the onset of fracture process driven by the crack interaction will occur in graphite-epoxy laminates for any parameters a/h, b/a and V_{0°=0.01…0.99 lying below those lines. Otherwise other mechanisms of fracture will occur.

4. Discussion

In this paper, the problem of modelling the onset of fracture process due to internal instability under static compression along layers has been studied for a laminar composite with a specific set of defects. Namely, a periodic array of coplanar interfacial cracks was investigated within the three-dimensional theory of stability, with each lamina of the material being treated as an individual three-dimensional object and boundary conditions, Eq. (7) and (8), satisfied at the interfaces. At that, the following assumptions have been imposed, which may cause some discrepancies between the current results and experimental data

The model of classical crack allows for interpenetration of crack faces, Eq. (7). However, in practical materials the crack faces *do* interact. The developed model should be extended in the future to the case of crack faces interaction. Internal instability does not always cause the

ultimate material failure. To fully study the problem of fracture of composites in compression, the postcritical behaviour must also be analysed.

Lamina was regarded as homogeneous transversely isotropic material. Hence, it was implicitly assumed that fibre distribution within the matrix is uniform (no resin rich regions were considered). For resin rich regions, distribution of strain/stresses is disturbed, thus it may trigger premature fibre microbuckling and subsequent kink band formation [15, 22].

Plane strain state was considered. This assumption is void in the vicinity of the traction free-edges of tested specimens. Furthermore stress concentrations near free-edge regions of multidirectional laminate may develop, due to stiffness discontinuities between adjacent plies, and may influence the stability of 0° layers and laminate failure. The magnitude and distribution of these through-thickness stresses depends on the laminate stacking sequence and ply orientation.

Fibre-fibre or fibre-free surface interaction was not considered in this paper. In practice, fibres within the matrix material do interact between each other and with the free surface of specimens, thus reducing the compressive strength of the composite, see [2].

Thermal expansion mismatch between fibres and matrix or between layers can induce compressive residual stresses development upon temperature change during manufacture [23-25]. Thus initial fibre waviness can appear in the fibrous composite which may advance or delay the onset of microbuckling/kink bands formation [26]. However, the residual stresses were not incorporated into the present model.

Practical composite materials may contain not only interlaminar, but also various sorts of intralaminar defects. The latter defects can be included in the analysis considering layers with reduced stiffness properties, see, for example, [27, 28]. Also, the presence of voids can greatly affect the shear strength of composite materials, and a number of studies indicate that

increasing void content also significantly decreases composite compressive strength, see [15] and references cited there.

6. Conclusions

The problem of instability of laminated graphite-epoxy composites in compression along periodic array of cracks was considered in this paper within the scope of the exact problem statement using the model of piecewise-homogeneous medium. The eigenvalue problem with respect to the controlled parameters was formulated for compressible, linear-elastic transversely isotropic layers and then solved using commercially available FE code ABAQUS 6.5 [16].

The two buckling instability regions were reported. The microcrack-like buckling region (the surface instability phenomenon), where the crack length (*a/h*) the crack spacing of two structural cracks (*b/a*) and the *0°*-plies volume fraction (V_{0°) do not influence the critical strain. Another is the region where parameters *(a/h), (b/a)* and (V_{0°) do influence the critical strain. In this case the internal stability loss phenomenon occurred.

Regardless the considered mode of stability loss the internal instability phenomenon occurs in the *0°*-plies and in the *90°*-plies for the low and the high volume fraction of *0°*-plies, respectively. The results for the *0°*-plies volume fraction $V_{0^\circ}<0.01$ and $V_{0^\circ}>0.99$ and the results for the model of two structural cracks converge for both considered buckling modes.

The shear mode of stability loss for the laminar composite contains a well pronounced extreme of the critical strain. Large decline of the critical strain is related to formation of the buckling band. The formation of the buckling band represents the transition between the internal instability in the *0°*-plies and in the *90°*-plies.

For the extensional mode of stability loss the internal instability phenomenon occurs in the 0°-plies for the layer volume fraction $V_{0^\circ}<0.4$ and in the 90°-plies for the layer volume fraction $V_{0^\circ}>0.6$. The critical strain level for the 0°-plies volume fraction $0.45<V_{0^\circ}<0.6$ increases rapidly due to change of the buckling region, from 0°-plies to 90°-plies. The influence of 0°-plies volume fraction $0.01<V_{0^\circ}<0.4$ and $0.7<V_{0^\circ}<0.99$ on the critical strain level is weak, and the results reasonably converge with the results for the model of two structural cracks.

For a very low volume fraction of 0°-plies and a very high volume fraction of 0°-plies the buckling pattern contains the series of isolated buckling regions, where two nearest cracks interacts.

References

1. Biot MA. Mechanics of Incremental Deformations. New York: Wiley, 1965.

2. Guz AN, (ed.). Micromechanics of Composite Materials: Focus on Ukrainian Research. Appl Mech Rev 1992;45(2):15-101.

3. Guz AN. Fundamentals of the Three-Dimensional Theory of Stability of Derormable Bodies, Berlin: Springer-Verlag, 1999.

4. Guz IA. Modelling of fracture for composites in compression along layers. Proc. 3rd International Conference on Modern Practice in Stress and Vibration Analysis, Dublin: 1997, pp.523-530.

5. Guz IA. Composites with interlaminar imperfections: substantiation of the bounds for failure parameters in compression. Compos Part B 1998;29B(4):343-350.

6. Guz IA, Soutis C. Critical strains in layered composites with interfacial defects loaded in uniaxial or biaxial compression. Plast Rubb Compos 2000;29(9):489-495.

7. Soutis C, Guz IA. Fracture of layered composites by internal fibre instability: Effect of interfacial adhesion. Aero J 2006;110(1105):185-195.

8. Soutis C, Guz IA. Predicting of fracture of layered composites coused by internal instability. Compos Part A; 2001;32(9):1243-1253.

9. Guz IA, Herrmann KP. On the lower bounds for critical loads under large deformations in non-linear hyperelastic composites with imperfect interlaminar adhesion. Euro J Mech A/Solids 2003;22(6):837-849.

10. Budiansky B, Fleck NA. Compressive kinking of fibre composites: a topical review. Appl Mech Rev 1994;47(6):S246-270.

11. Soutis C. Failure of notched CFRP laminates due to fibre microbuckling: a topical review. J Mech Behav Mater 1996;6(4):309-330.

12. Guz AN, Rodger AA, Guz IA. Developing compressive failure theory for nanocomposites. Int Appl Mech 2005;41(3):233-255.

13. Soutis C, Turkmen D. Moisture and temperature effects of the compressive failure of CFRP unidirectional laminates. J Compos Mater 1997;31(8):832–849.

14. Niu K. Talreja R. Modeling of compressive failure in fiber reinforced composites. Int J Solids Struct 2000;37(17):2405-2428.

15. Waas AM, Schultheisz CR. Compressive failure of composites, Part I and Part II. Prog Aero Sci 1996;32:1-78.

16. Abaqus 6.5 user manuals

17. Fung YC, Tong Pin. Classical and computional solid mechanics, Advanced series in engineering science, vol.1, Singapore: World Scientific Publishing, 2001.

18. Winiarski B, Guz IA. The effect of cracks interaction on the critical strain in orthotropic heterogeneous materials under compressive static loading. Proceedings of ASME

International Mechanical Engineering Congress and Exposition, Chicago, Illinois, USA: ASME, 2006.

19. Winiarski B, Guz IA. Plane problem for layered composites with periodic array of interfacial cracks under compressive static loading. Int J Fract 2007;144(2):113-119.

20. Guz AN, Guz IA. Analytical solution of stability problem for two composite half-planes compressed along interfacial cracks. Compos Part B 2000;31(5):405-418.

21. Peters ST, (ed.). Handbook of composites, II ed., London: Chapman & Hall, 1998.

22. Guynn EG, Ochoa OO, Bradley WL. A parametric study of variables that affect fiber microbuckling initiation in composite laminates: Part 1 – Analysis. Part 2 – Experiment. J Compos Mater 1992;26(11):1594-1643.

23. Wisnom MR, Gigliotti M, Ersoy N, Campbell M, Potter KD. Mechanisms generating residual stresses and distortion during manufacture of polymer–matrix composite structures. Compos Part A 2006;37(4):522-529.

24. Parlevliet PP, Bersee HEN, Beukers A. Residual stresses in thermoplastic composites—A study of the literature - Part I: Formation of residual stresses. Compos Part A 2006;37(11):1847-1857.

25. Parlevliet PP, Bersee HEN, Beukers A. Residual stresses in thermoplastic composites—A study of the literature - Part II: Experimental techniques. Compos Part A 2007;38(3):651-665.

26. Jensen HM. Residual stress effects on the compressive strength of uni-directional fibre composites Acta Mater 2002;50(11):2895-2904.

27. Zhang J, Herrmann KP. Stiffness degradation induced by multilayer intralaminar cracking in composite laminates, Compos Part A 1999;30(5):683-706.

28. Kashtalyan M, Soutis C. Mechanisms of internal damage and their effect on the behavior and properties of cross-ply composite laminates. Int Appl Mech 2002;38(6):641-657.

Table 1. The mechanical properties of the graphite-epoxy lamina [10].

The fibre volume fraction in each layer is 0.6.

part	E_{11} [GPa]	E_{22} [GPa]	E_{33} [GPa]	ν_{12}	ν_{13}	ν_{23}	G_{12} [GPa]	G_{13} [GPa]	G_{23} [GPa]
C	12.5	155	12.5	0.019	0.458	0.248	4.4	3.2	4.4
L, R	12.5	12.5	155	0.458	0.019	0.019	3.2	4.4	4.4

Table 2. The number of elements for V_0=0.5; and for V_0=0.01 in parentheses.

Crack length	*a/h*	*b/a*	Number of elements		
			Part L	Part C	Part R
a/h ≥ 1	1 (1)	0 (0)	721 (4959)	1081 (1208)	721 (4985)
	4 (10)	5 (0.95)	3274 (24242)	5067 (8956)	3172 (24943)
a/h < 1	0.8 (0.8)	0 (0)	1457 (6306)	2325 (3330)	1471 (6286)
	0.1 (0.1)	0 (1.1)	10084 (17456)	19316 (14143)	9992 (17389)

Figure Captions

Figure 1. The representative volume element: (a) for the periodic array of cracks, (b) for structural cracks located on the different coplanar interfaces.

Figure 2. The mesh pattern in the vicinity of cracks*; a/h*=5*, b/a*= 0*; V_0*=0.25.

Figure 3. The shear mode for a graphite-epoxy composite. The results of FEA for critical strains are shown by solid lines for the crack length *a/h* = 1, 15; and the crack spacing *b/a* = 0, 0.8. Experimental critical strain is shown by dashed lines for the transverse direction (1.53%) and along the fibres (1.06%). The dashed-dotted line gives the analytical solution [3] for the case of microcrack.

Figure 4. The extensional mode for a graphite-epoxy composite. The results of FEA for critical strains are shown by solid lines for the crack length *a/h* = 1, 15; and the crack spacing *b/a* = 0, 0.8. Experimental critical strain is shown by dashed lines for the transverse direction (1.53%) and along the fibres (1.06%). The dashed-dotted line gives the analytical solution [3] for the case of microcrack.

Figure 5. FEA results for the shear mode for a graphite-epoxy composite; maximum in-plane principal strain distributions for V_0=0.01*, b/a*=0.8*, a/h*=20. The buckling pattern at ε_{cr}=1.5% contains the series of isolated buckling regions.

Figure 6. FEA results for the shear mode for a graphite-epoxy composite; maximum in-plane principal strain distributions for V_{0f}=0.5, *b/a*=0.8, *a/h*=5. The formation of the microbuckling band due to multiple crack interaction at ε_{cr}=1.38%.

Figure 7. FEA results for the extensional mode for a graphite-epoxy composite; maximum in-plane principal strain distributions for V_{0f}=0.2, *b/a*=0.8, *a/h*=7. The buckling pattern at ε_{cr}=2.08% contains the series of isolated buckling regions.

Figure 8. FEA results for the extensional mode for a graphite-epoxy composite: (a) maximum in-plane principal strain distributions for V_{0f}=0.4, *b/a*=0, *a/h*=9. The internal instability occurs in the *0°*-plies at ε_{cr}=0.9%; (b) maximum in-plane principal strain distributions for V_{0f}=0.6, *b/a*=0, *a/h*=9. The internal instability occurs in the *90°*-plies at ε_{cr}=2.72%.

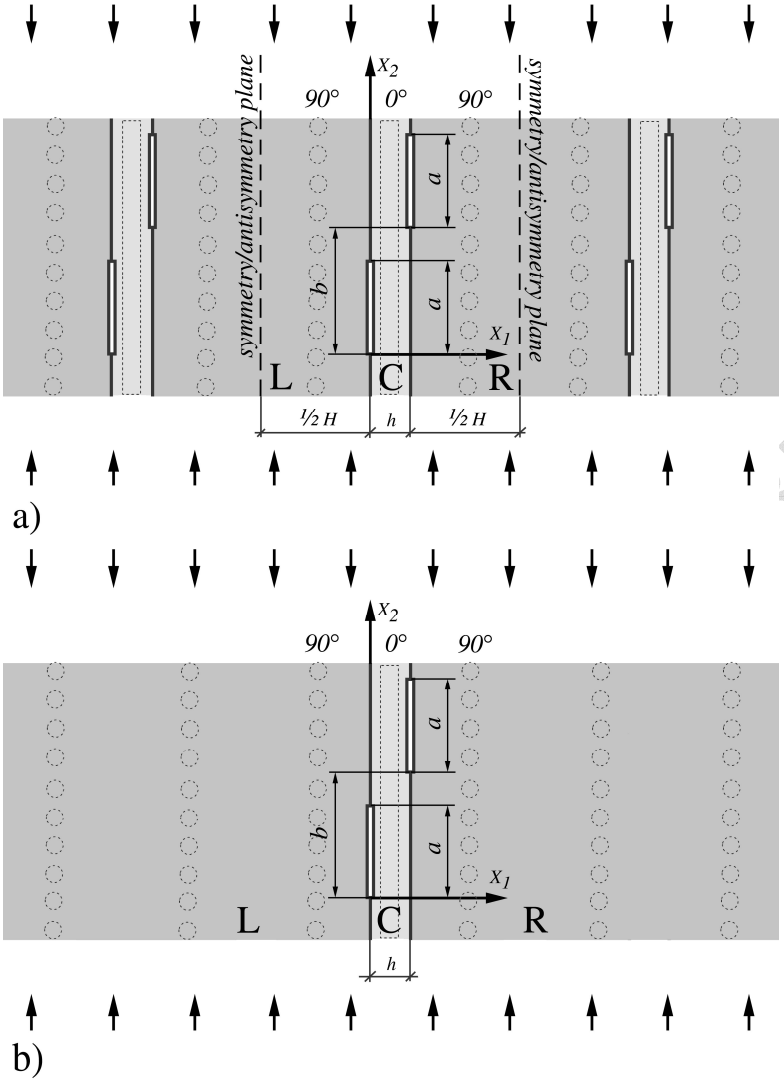

Figure 1.

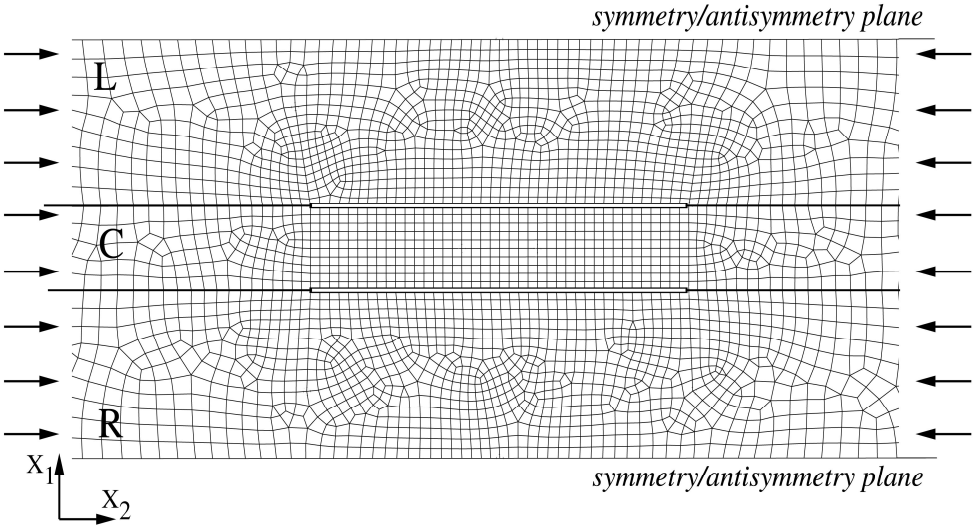

Figure 2.

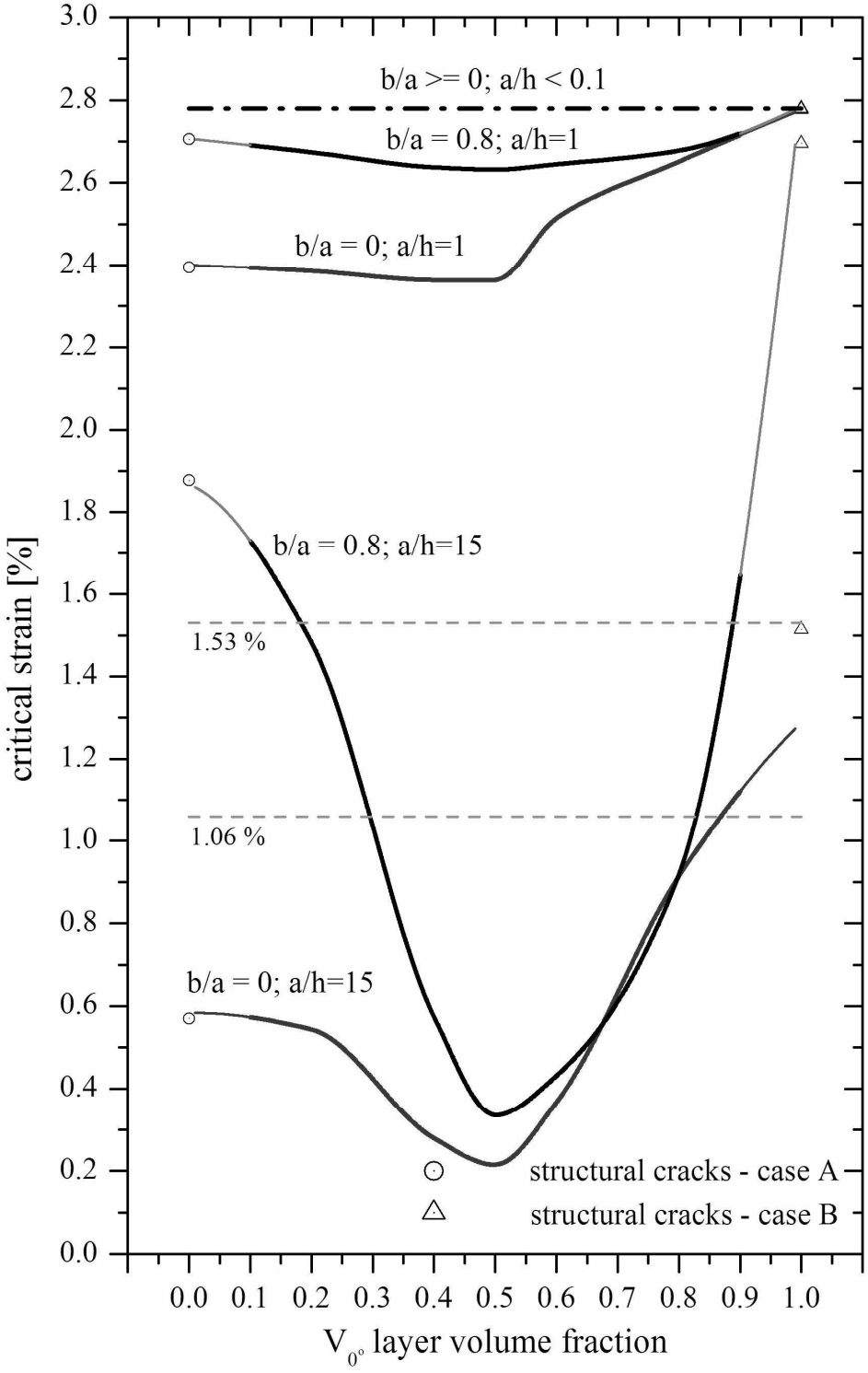
b/a >= 0; a/h < 0.1
b/a = 0.8; a/h=1
b/a = 0; a/h=1
b/a = 0.8; a/h=15
b/a = 0; a/h=15
1.53 %
1.06 %
structural cracks - case A
structural cracks - case B
critical strain [%]
V0° layer volume fraction
3.0
2.8
2.6
2.4
2.2
2.0
1.8
1.6
1.4
1.2
1.0
0.8
0.6
0.4
0.2
0.0
0.0 0.1 0.2 0.3 0.4 0.5 0.6 0.7 0.8 0.9 1.0

Figure 3.

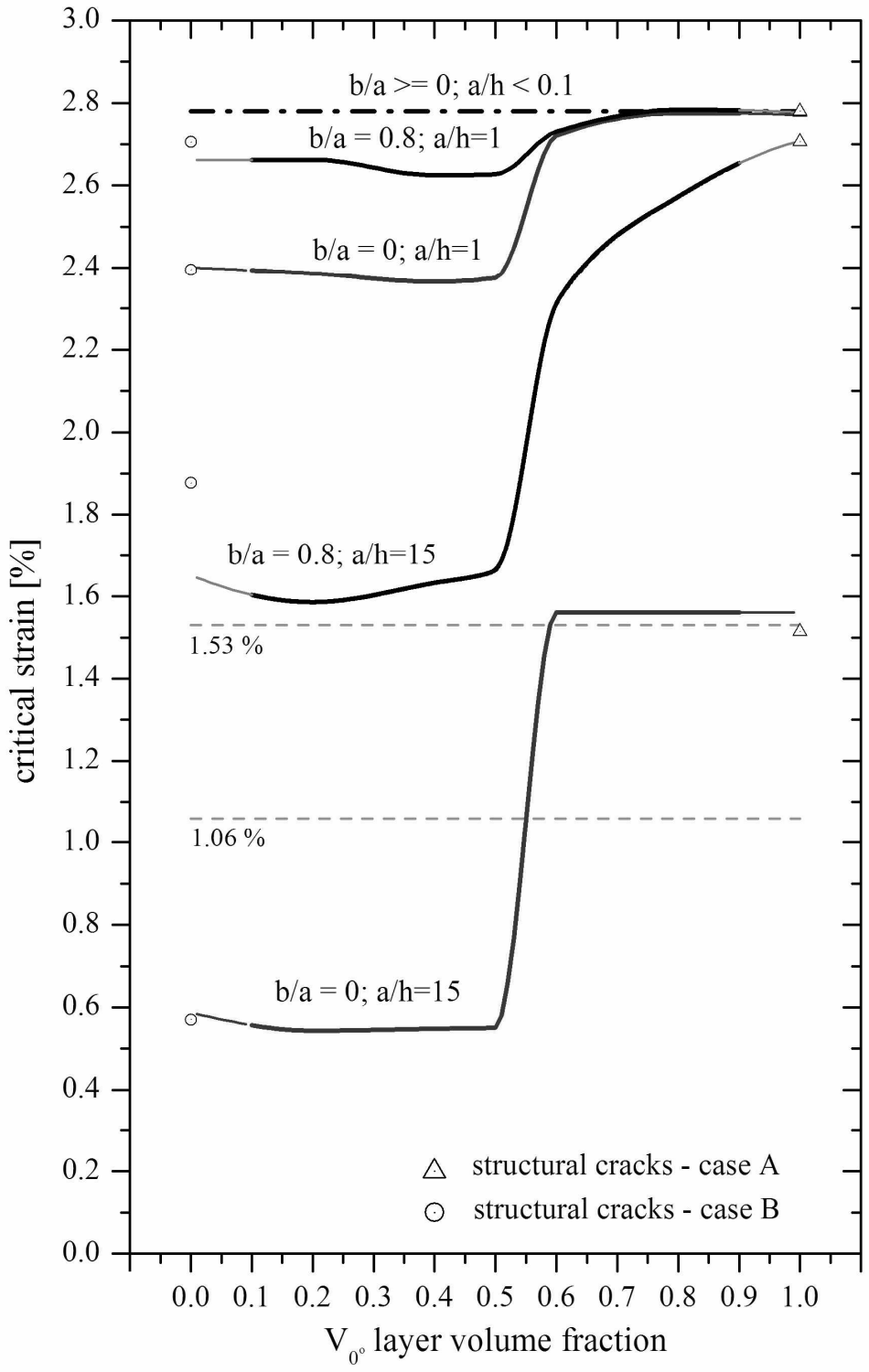
b/a >= 0; a/h < 0.1
b/a = 0.8; a/h=1
b/a = 0; a/h=1
b/a = 0.8; a/h=15
b/a = 0; a/h=15
1.53 %
1.06 %
structural cracks - case A
structural cracks - case B
critical strain [%]
V0° layer volume fraction
3.0
2.8
2.6
2.4
2.2
2.0
1.8
1.6
1.4
1.2
1.0
0.8
0.6
0.4
0.2
0.0
0.0 0.1 0.2 0.3 0.4 0.5 0.6 0.7 0.8 0.9 1.0

Figure 4.

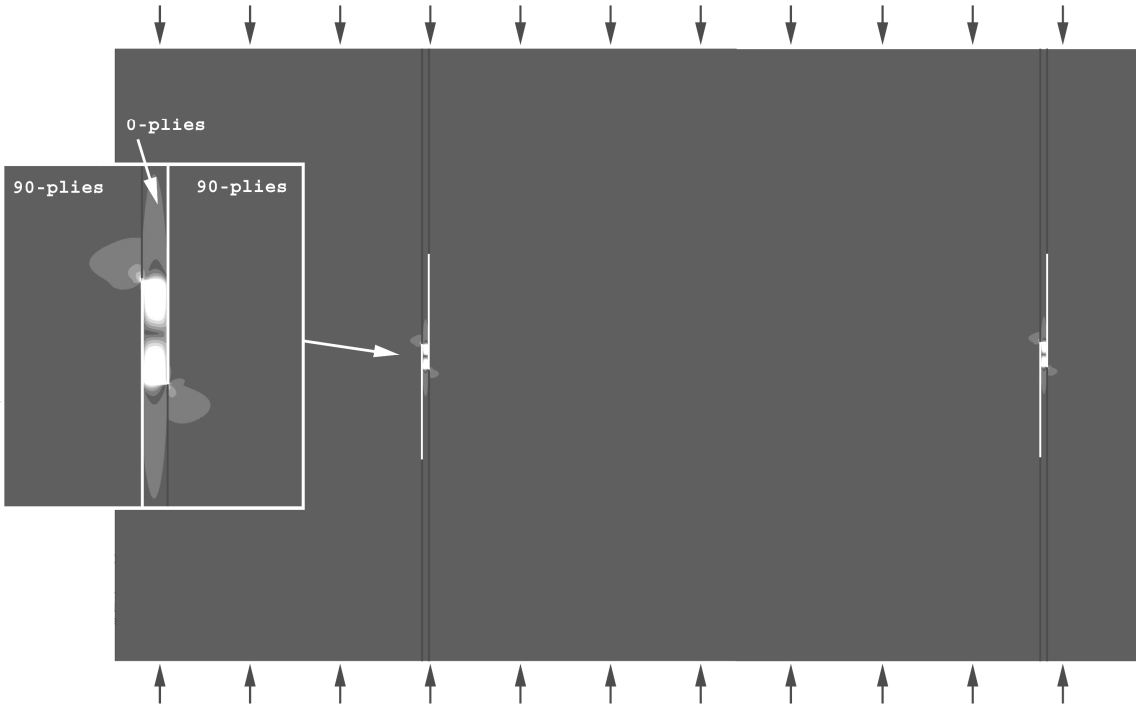

Figure 5.

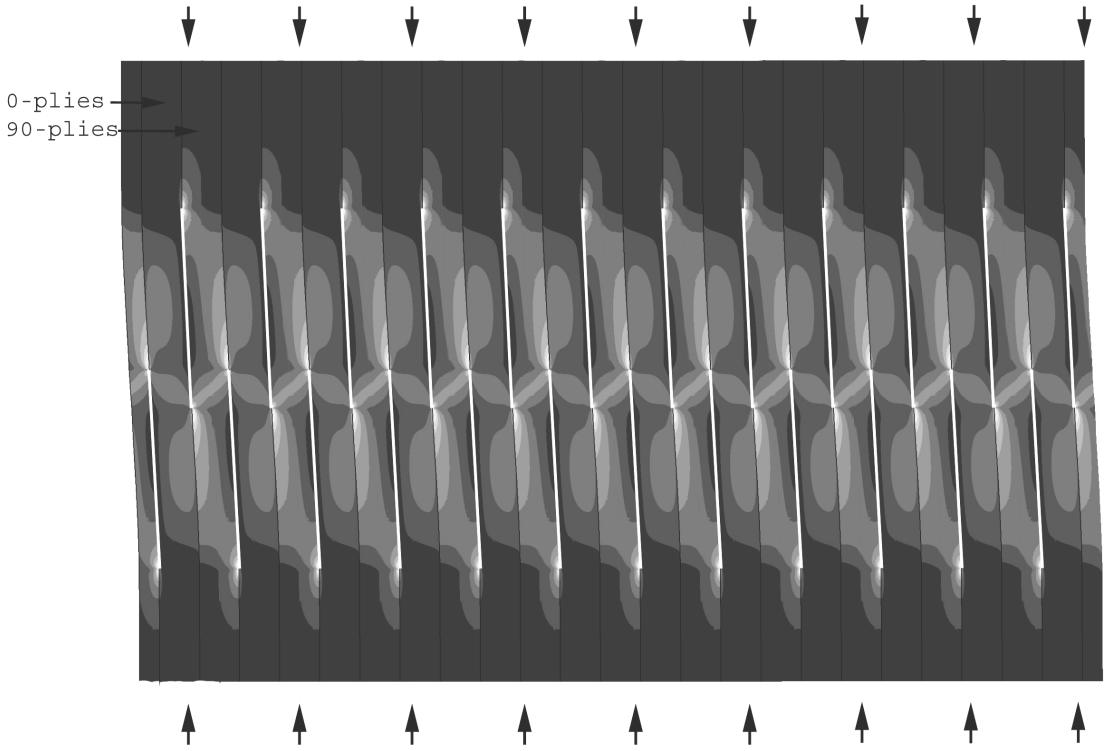

Figure 6.

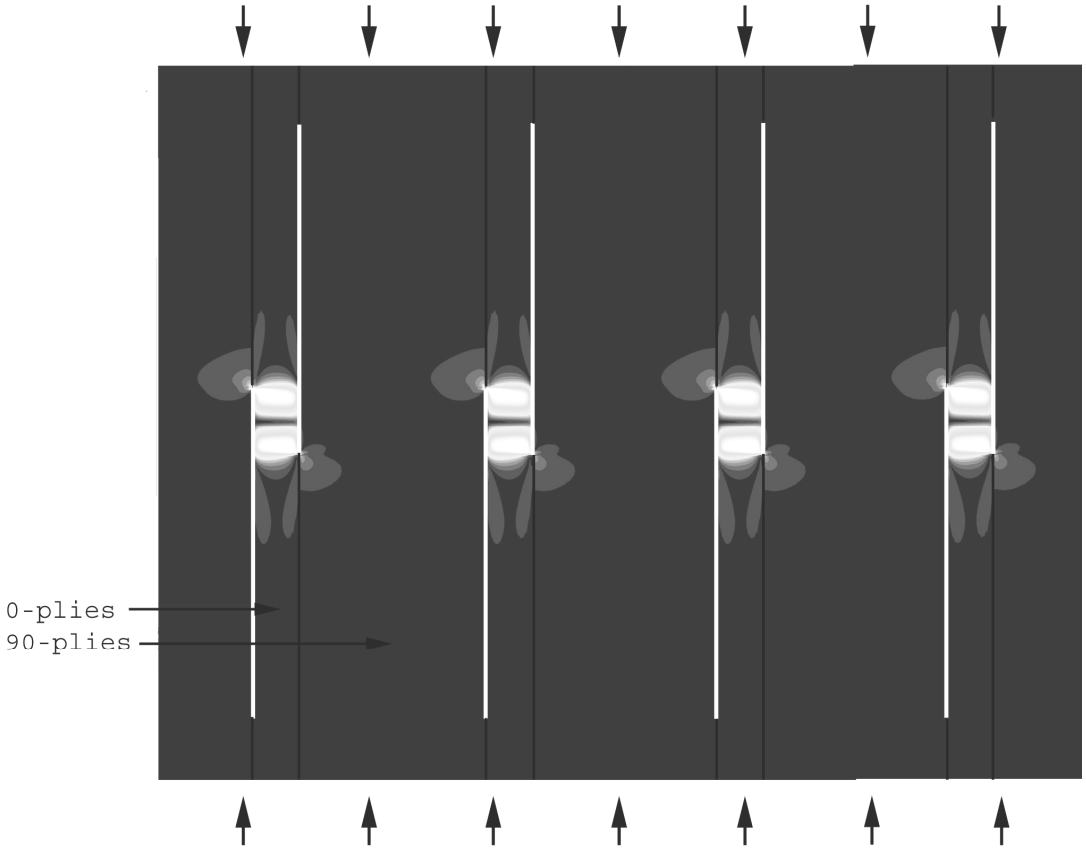

Figure 7.

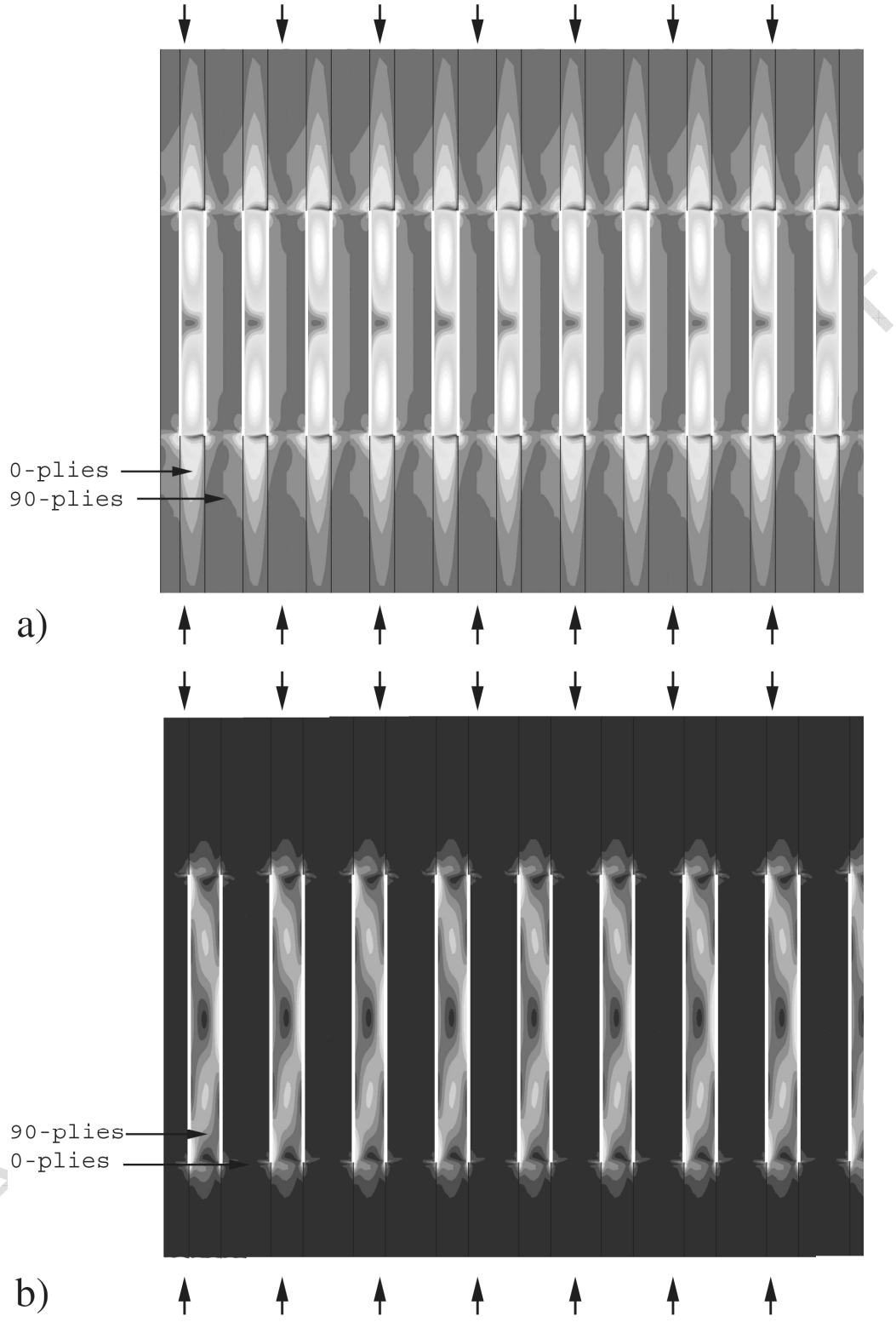

Figure 8.